



Contents lists available at ScienceDirect

## Bioorganic &amp; Medicinal Chemistry Letters

journal homepage: [www.elsevier.com/locate/bmcl](http://www.elsevier.com/locate/bmcl)

## Discovery of potent 1*H*-imidazo[4,5-*b*]pyridine-based c-Met kinase inhibitors via mechanism-directed structural optimization



Xiao-De An<sup>a,b,†</sup>, Hongyan Liu<sup>b,†</sup>, Zhong-Liang Xu<sup>b</sup>, Yi Jin<sup>c</sup>, Xia Peng<sup>b</sup>, Ying-Ming Yao<sup>a,\*</sup>, Meiyu Geng<sup>b,\*</sup>, Ya-Qiu Long<sup>b,\*</sup>

<sup>a</sup> Key Laboratory of Organic Synthesis of Jiangsu Province, College of Chemistry, Chemical Engineering and Materials Science, Soochow University, Suzhou 215123, China

<sup>b</sup> State Key Laboratory of Drug Research, Shanghai Institute of Materia Medica, Chinese Academy of Sciences, Shanghai 201203, China

<sup>c</sup> School of Chemical Science and Technology, Yunnan University, Kunming 650091, China

## ARTICLE INFO

## Article history:

Received 4 November 2014

Revised 24 November 2014

Accepted 26 November 2014

Available online 4 December 2014

## Keywords:

c-Met tyrosine kinase

Small molecule inhibitor

Imidazonaphthyridinone

Imidazopyridine

Binding mode

Pyridone-3-carboxamide

Cyclopropane-1,1-dicarboxamide

## ABSTRACT

Starting from our previously identified novel c-Met kinase inhibitors bearing 1*H*-imidazo[4,5-*h*][1,6]naphthyridin-2(3*H*)-one scaffold, a global structural exploration was conducted to furnish an optimal binding motif for further development, directed by the enzyme inhibitory mechanism. First round SAR study picked two imidazonaphthyridinone frameworks with 1,8- and 3,5-disubstitution pattern as class I and class II c-Met kinase inhibitors, respectively. Further structural optimization on type II inhibitors by truncation of the imidazonaphthyridinone core and incorporation of an *N*-phenyl cyclopropane-1,1-dicarboxamide pharmacophore led to the discovery of novel imidazopyridine-based c-Met kinase inhibitors, displaying nanomolar enzyme inhibitory activity and improved Met kinase selectivity. More significantly, the new chemotype c-Met kinase inhibitors effectively inhibited Met phosphorylation and its downstream signaling as well as the proliferation of Met-dependent EBC-1 human lung cancer cells at submicromolar concentrations.

© 2014 Elsevier Ltd. All rights reserved.

The MET tyrosine kinase is a cell surface receptor for the hepatocyte growth factor (HGF), a pleiotropic cytokine controlling pro-migratory, anti-apoptotic and mitogenic signals.<sup>1–4</sup> Normal activation of c-Met kinase is essential for wound healing and embryonic development.<sup>2</sup> Aberrant c-Met due to specific genetic lesions, including transcriptional upregulation, gene amplification, activating mutations, increased autocrine or paracrine ligand mediated stimulation, occurred in many types of cancers.<sup>5</sup> Importantly, deregulated c-Met activation has been associated with poor clinical outcomes.<sup>6,7</sup> Furthermore, compelling evidence has linked c-Met overactivation to mediating intrinsic or acquired resistance to targeted therapies.<sup>8,9</sup> All of these emphasize c-Met as an attractive target for cancer therapy. Indeed, quite a few c-Met inhibitors are now under clinical investment, which further proved the feasibility of c-Met inhibition method in cancer therapy.

In the past decade, an impressive number of small molecule c-Met inhibitors have been reported,<sup>10–14</sup> which have basically been categorized into two classes based on their structure and binding modes in the c-Met kinase domain.<sup>2,15</sup> Type I inhibitors bind in a

U-shaped conformation to the ATP-binding site at the entrance of the kinase pocket and wrap around Met1211, while type II inhibitors bind to c-Met with an extended conformation that stretches from the ATP-binding site (hinge region) to the deep hydrophobic Ile 1145 pocket near the C-helix region. Some representative chemical structures from each class are illustrated in Figure 1. In general, type I inhibitors block c-Met kinase activity with high selectivity against other kinases, whereas a majority of type II molecules are multikinase inhibitors, but expected to be more effective against the mutations of c-Met active site that disrupt the type I binding mode.<sup>16,17</sup>

Recently, we identified a new class of type II c-Met kinase inhibitors with 1,3,5-trisubstituted-1*H*-imidazo[4,5-*h*][1,6]naphthyridin-2(3*H*)-one scaffold (Fig. 2, exemplified by LXM-22), by employing drug repurposing and pharmacophore incorporation strategies.<sup>18</sup> The new scaffold inhibitors displayed promising pharmacological property and cellular efficacy, but the inhibitory activity fell in micromolar range. According to the binding mode predicted by molecular modeling,<sup>18</sup> the 1*H*-imidazo[4,5-*h*][1,6]naphthyridin-2(3*H*)-one-based c-Met kinase inhibitor adopts an extended conformation in the ATP-binding pocket of the enzyme with the activation loop in an inactive, DFG-out conformation. However, the heterotricyclic core resides in the middle of the channel between the hinge region and the DFG motif,

\* Corresponding authors. Tel./fax: +86 21 50806876.

E-mail addresses: [yaoym@suda.edu.cn](mailto:yaoym@suda.edu.cn) (Y.-M. Yao), [mygeng@simm.ac.cn](mailto:mygeng@simm.ac.cn) (M. Geng), [yqiong@simm.ac.cn](mailto:yqiong@simm.ac.cn) (Y.-Q. Long).

† These authors contributed to this work equally.

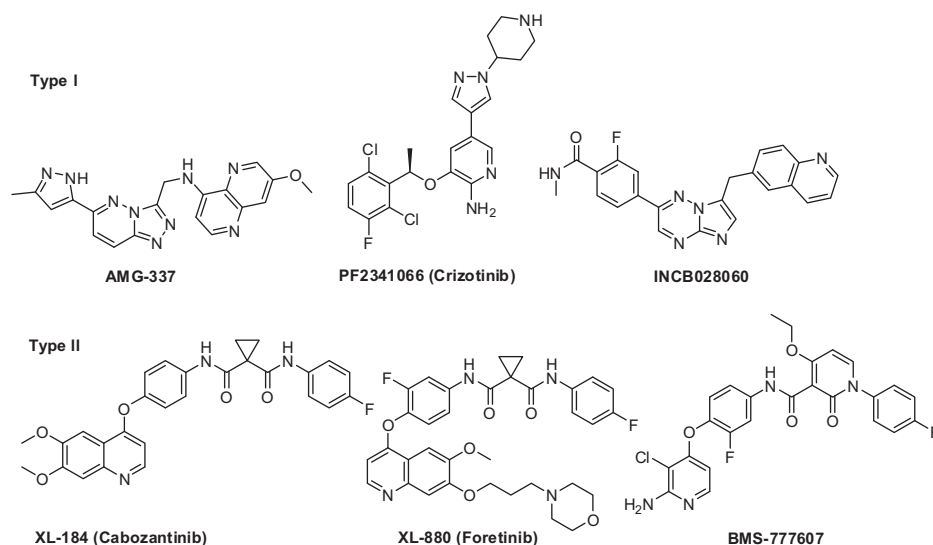


**Figure 1.** Representative structures of type I and type II c-Met kinase inhibitors launched or under clinical trials.

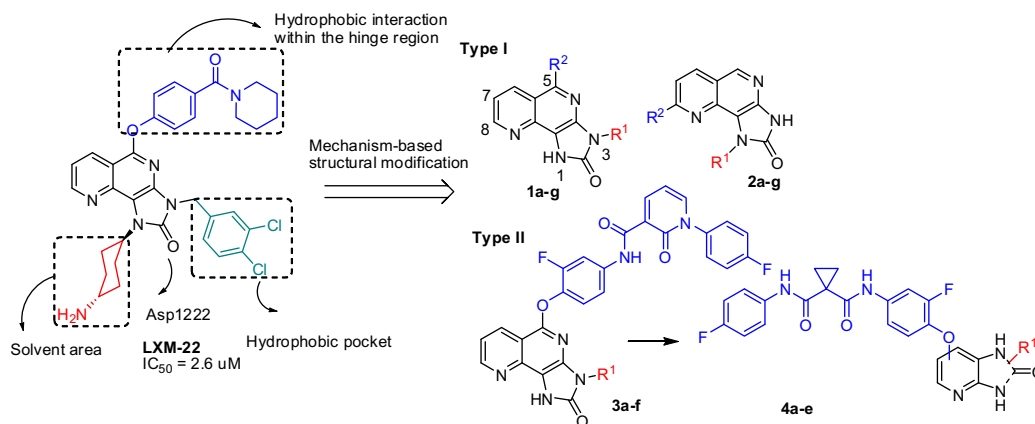


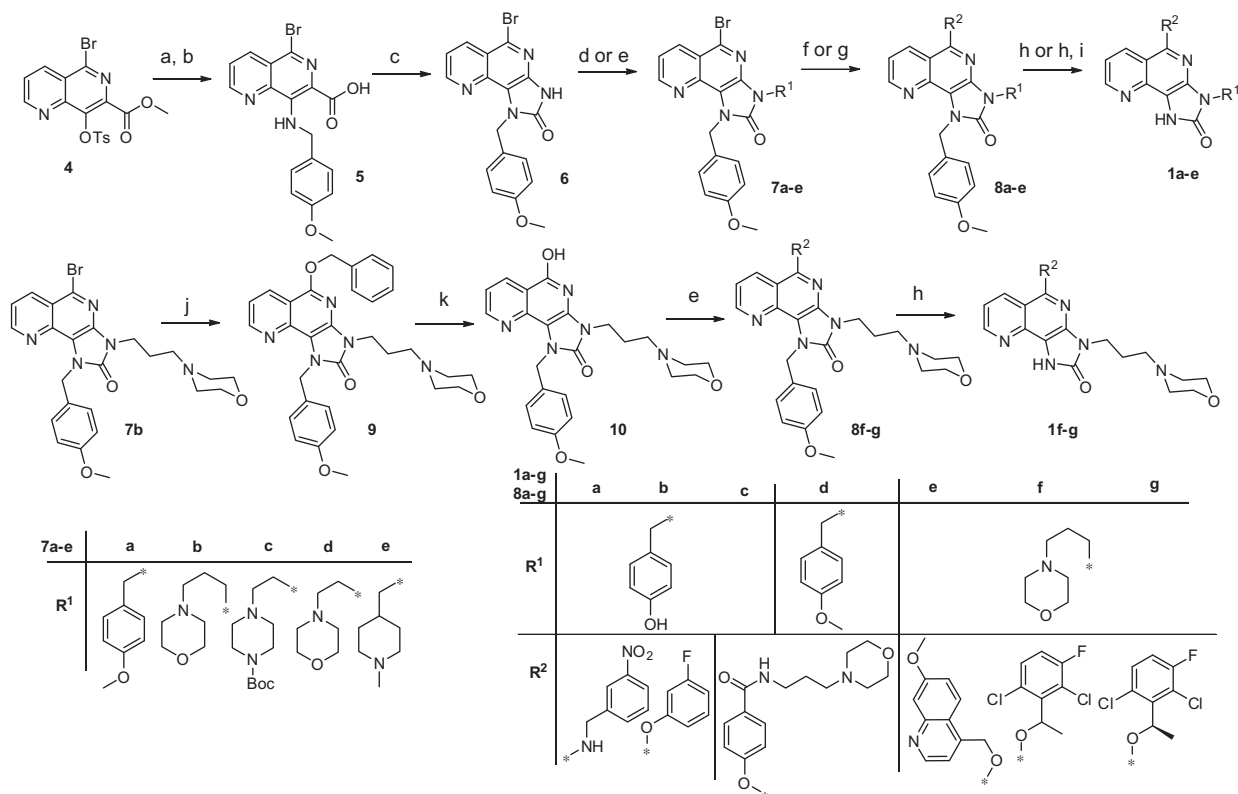
**Figure 2.** The mechanism-based structural optimization on the 1*H*-imidazo[4,5-*h*][1,6]naphthyridin-2(3*H*)-one scaffold to develop novel type I and II c-Met kinase inhibitors.

due to the bulky size, thus losing the key hydrogen bonding interactions with Met1160. Herein, we tried to improve the potency of imidazonaphthyridinone c-Met inhibitors based on the inhibitory mechanism through two approaches: one is evolved into type I inhibitor by using the 1*H*-imidazo[4,5-*h*][1,6]naphthyridin-2(3*H*)-one as a U-shape inducing moiety with two proper substituents deep into the solvent and hydrophobic regions, respectively (Fig. 2, **1a–g**, **2a–g**); the other is optimized into a bona fide type II inhibitor by incorporating the typical pharmacophore of *N*<sup>1</sup>-phenyl-*N*<sup>3</sup>-(4-fluorophenyl)malonamide or its bioisostere<sup>19</sup> and further truncation of the core structure to fit the ATP binding site and DFG motif pocket (Fig. 2, **3a–f**, **4a–e**).

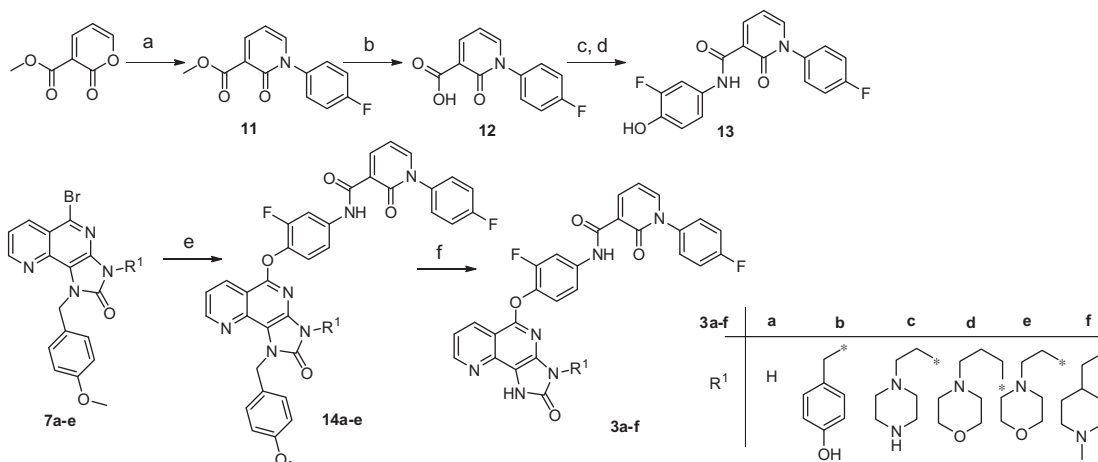
With respect to the U-shaped type I inhibitor design, the optimal substitution pattern was investigated by synthesizing 3,5- and 1,8-disubstituted analogs with hydrophobic and hydrophilic groups incorporated rotationally at the two positions (**1a–g**, and **2a–g**). As shown in Scheme 1, starting from the 1,6-naphthyridine precursor, which was prepared according to the known procedure,<sup>20</sup> the introduction of the 4-methoxybenzylamino group to 8-position was readily realized by the aromatic nucleophilic substitution of 4-methoxybenzylamine. Then the 1*H*-imidazol-2(3*H*)-one core was constructed in a similar manner as we previously reported,<sup>18</sup> whereby the Curtius rearrangement produced an isocyanate and the following attack of the neighboring 8-amino

group furnished the cyclic urea **6**. However, the approach to install the 3-substituent was dependent on the structure of the coupling partner. Mitsunobu reaction and nucleophilic substitution reaction were applied for an alcohol and a halide to convert the 1*H*-imidazol-2(3*H*)-one compound **6** into 1,3-disubstituted intermediates **7(b, d, e)** and **7(a, c)**, respectively. Further introduction of 5-substituent was achieved via Williamson etherification reaction between 5-bromo intermediates **7** and the corresponding alcohols to yield **8b–e** or Buchwald–Hartwig cross coupling with amines to give **8a**. The removal of the *N*<sup>1</sup>-4-methoxybenzyl group by TFA and TfOH mixture and further demethylation by BBr<sub>3</sub> afforded the designed 3,5-disubstituted 1*H*-imidazo[4,5-*h*][1,6]naphthyridin-2(3*H*)-one derivatives **1a–e**. Interestingly, by tuning the ratio of TfOH and TFA ranging from 10% to 50%, selective debenzoylation on the *N*<sup>1</sup>-position without impacting *N*<sup>3</sup>-benzyl group was achieved. Notably, when a privileged structure of 1-(2,6-dichloro-3-fluorophenyl)ethoxy group was installed at 5-position, a different synthetic route was employed. The 5-bromo intermediate **7b** was converted into a phenol **10**, followed by Mitsunobu reaction with 1-(2,6-dichloro-3-fluorophenyl)ethanol to generate **1f–g**.

As shown in Scheme 2, the 3,5-disubstituted type II inhibitors **3a–f** were synthesized similarly, just appending a specified structure of *N*-(3-fluoro-4-(oxyphenyl)-1-(4-fluorophenyl)-2-oxo-1,2-dihydropyridine-3-carboxamide) at 5-position via Williamson



**Scheme 1.** Reagent and conditions: (a) 4-methoxybenzylamine, TEA, THF, 60 °C, 10 h, 83% yield; (b) 2 N LiOH (aq), THF, 50 °C, 12 h, 74% yield; (c) DPPA, toluene, TEA, 100 °C, 10 h, 38% yield; (d) 4-methoxybenzyl chloride or *tert*-butyl 4-(2-bromoethyl)piperazine-1-carboxylate, K<sub>2</sub>CO<sub>3</sub>, DMF, rt–70 °C, 10–20 h (for **7a,7c**); (e) ROH, DEAD, PPh<sub>3</sub>, THF, rt, 3 h (for **7b, 7d, 7e**); (f) ROH, K<sub>2</sub>CO<sub>3</sub>, DMF, 110 °C, 1 h; (g) 1-(aminomethyl)-3-nitrobenzene, Pd(OAc)<sub>2</sub>, dimethylbis(diphenyl)phosphinoxanthene, Cs<sub>2</sub>CO<sub>3</sub>, 1,4-dioxane, 80 °C, 2 h, 36% yield; (h) TFOH : TFA = 10–50%, rt; (i) BBr<sub>3</sub>, DCM, 0 °C–rt, 4 h; (j) benzyl alcohol, NaH, DMF, rt, 40 min; (k) H<sub>2</sub>, Pd–C, rt, 30 min, 80% yield.



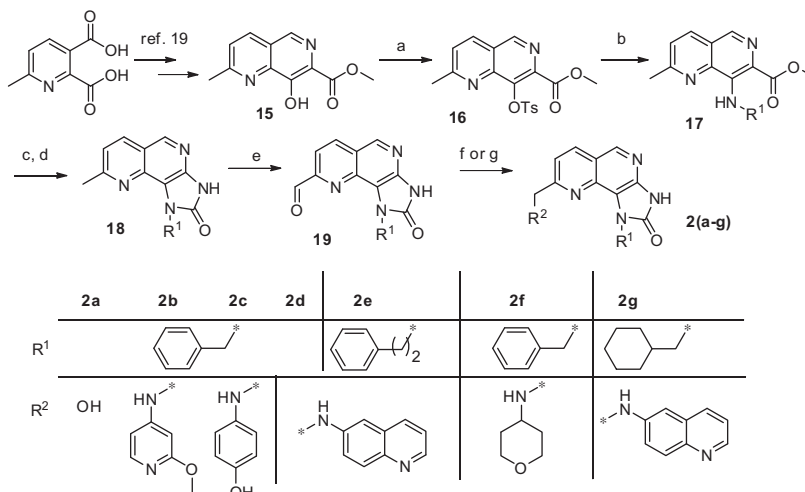
**Scheme 2.** Reagent and conditions: (a) 4-fluoroaniline, EDCI, DMAP, DMF, rt, 10 h, 65% yield. (b) 2 N NaOH (aq), rt, 3 h. (c) SOCl<sub>2</sub>, CH<sub>2</sub>Cl<sub>2</sub>, cat. DMF, reflux, 3 h. (d) 4-Amino-2-fluorophenol, K<sub>2</sub>CO<sub>3</sub>, rt, 10 h, 30% overall yield for two steps. (e) **13**, K<sub>2</sub>CO<sub>3</sub>, DMF, 110 °C, 1 h; (f) TFOH : TFA = 10–50%, rt.

etherification reaction. This fragment was recognized as a typical pharmacophore for type II *c*-Met inhibitors and was prepared according to the literature method.<sup>21</sup>

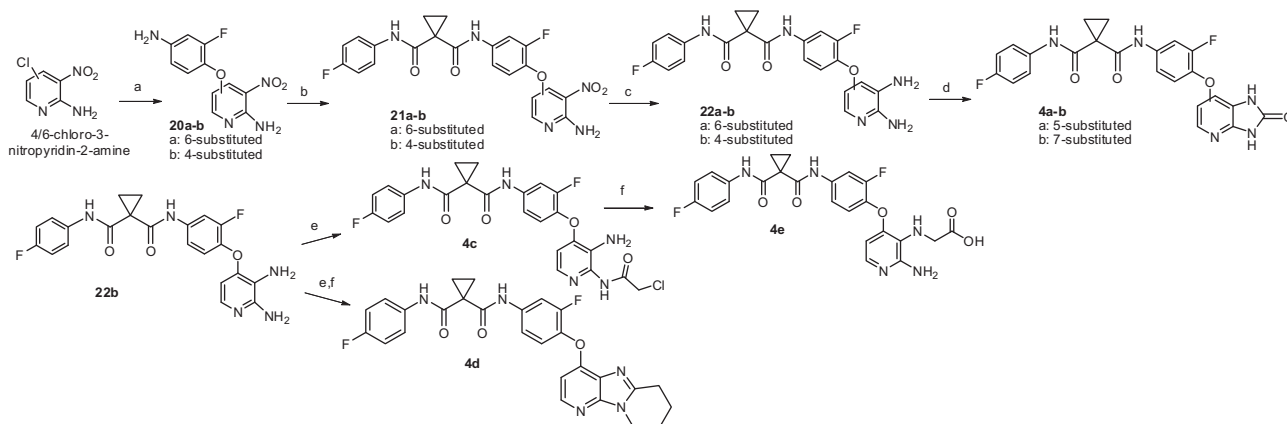
For the synthesis of 1,8-disubstituted-1*H*-imidazo[4,5-*h*][1,6]naphthyridin-2(3*H*)-one derivatives, as described in [Scheme 3](#), see 6-methylpyridine-2,3-dicarboxylic acid was used as the starting material subjected to the same procedures as pyridine-2,3-dicarboxylic acid, affording the key intermediate of 8-methyl-1*H*-imidazo[4,5-*h*][1,6]naphthyridin-2(3*H*)-one **18**.<sup>20</sup> Oxidation with SeO<sub>2</sub> produced aldehyde **19** to undergo a reduction or

reductive amination reaction, furnishing the 8-substituted target compounds **2a–g**.

Further truncated analogs (**4a–d**) were synthesized from 4/6-chloro-3-nitropyridine-2-amine, as depicted in [Scheme 4](#). Nucleophilic substitution by aminophenol followed by amidation enabled the incorporation of *N*-(3-fluoro-4-hydroxyphenyl)-*N*-(4-fluorophenyl)cyclopropane-1,1-dicarboxamide (**21a–b**). Reduction of the nitro group by sodium borohydride in the presence of nickel chloride afforded the pyridine-2,3-diamine key intermediate (**22a–b**), which was converted to the 1*H*-imidazo[4,5-*b*]pyridin-2(3*H*)-one



**Scheme 3.** Reagent and conditions: (a) TsCl, DCM, 60 °C, 2 h, 74% yield; (b) amines, TEA, THF, 100 °C, 10 h; (c) 2 N LiOH (aq), THF, 50 °C, 12 h; (d) DPPA, toluene, TEA, 80 °C, 6 h; (e) SeO<sub>2</sub>, 1,4-dioxane, 75–100 °C, 3 h; (f) NaBH<sub>4</sub>, ethanol, ice-salt, 10 min (for the synthesis of **2a**), 70% yield; (g) RNH<sub>2</sub>, NaBH<sub>3</sub>CN, CH<sub>3</sub>OH, CH<sub>3</sub>COOH, anhydrous MgSO<sub>4</sub>, rt, 2 h; (h) 2-(trimethylsilyl)-phenyltrifluoromethanesulfonate, CsF, CH<sub>3</sub>CN, 40 °C, 48 h, 43% yield.



**Scheme 4.** Reagents and conditions: (a) 4-amino-2-fluorophenol, *t*-BuOK, DMF, 80 °C, N<sub>2</sub>, 80–85% yield; (b) 1-((4-fluorophenyl)carbamoyl)cyclopropanecarboxylic acid, HOBT, EDC, DIEA, DMF, rt, 74–80% yield; (c) NiCl<sub>2</sub>·6H<sub>2</sub>O, THF/MeOH (v:v = 1:1), NaBH<sub>4</sub>, 0 °C, 85–92% yield; (d) bis(trichloromethyl)carbonate, cat. DMF, THF, 0 °C, 85–90% yield; (e) 2-chloroacetyl chloride (for the preparation of **4c**, 87% yield) or 5-bromopentanoyl chloride (for the preparation of **4d**, yield 29%), TEA, THF, 0 °C; (f) AcOH, 110 °C, 43% yield.

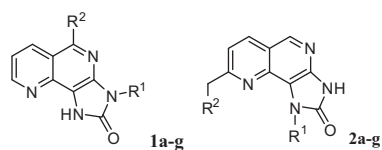
derivatives (**4a–b**) by reaction with bis(trichloromethyl)carbonate. Treatment of the pyridine-2,3-diamine intermediate with haloalkanoyl chloride delivered the 6,7,8,9-tetrahydroimidazo[1,2-*a*:5,4-*b'*]dipyridine analog (**4d**) and the aminopyridine derivatives (**4c**, **4e**).

All the synthesized 1*H*-imidazo[4,5-*h*][1,6]naphthyridin-2(3*H*)-one derivatives were evaluated with the *c*-Met kinase inhibition. An initial SAR study was focused on an optimal binding motif exploration. For the designed type I inhibitors using imidazonaphthyridinone as the U-shape inducing module, both 3,5-disubstitution and 1,8-disubstitution pattern proved unfavorable for binding to *c*-Met kinase domain, with the latter being slightly more advantageous. As shown in Table 1, most of the 3,5-disubstituted 1*H*-imidazo[4,5-*h*][1,6]naphthyridin-2(3*H*)-one derivatives (**1a–g**) exhibited weak to moderate inhibition against Met enzyme, even though the privileged structures were incorporated into N-3 and C-5 positions. We selected isopropyl morpholine or phenol as the hydrophilic substituent and the benzene or heteroaromatic ring as the hydrophobic group since they were frequently found in potent *c*-Met inhibitors.<sup>22,23</sup> The best compound in this series was exemplified by **1c** with hydrophobic group at N-3 and hydrophilic group at C-5 position (**1c**, IC<sub>50</sub> = 26 μM). On the other

hand, the 1,8-disubstitution pattern with a heteroaromatic or hydrophilic moiety at C-8 position and the hydrophobic group at N-1 position turned out more effective for the Met kinase inhibition (Table 1, **2a–g**). When benzyl group was installed at N-1 position and 2-methoxypyridin-4-amino or quinolin-6-amino group at C-8 position, the resulting 1,8-disubstituted imidazonaphthyridinone derivatives displayed low micromolar inhibition against *c*-Met enzyme (**2b**, IC<sub>50</sub> = 3.9 μM; **2d**, IC<sub>50</sub> = 12.7 μM). The extension of the phenyl ring by one more methylene from N-1 position (**2e**), or the replacement of the aromatic or heteroaromatic ring at position N-1 or C-8 by aliphatic ring (**2f**) or heterocycle (**2g**) abolished the Met inhibitory activity, indicating the important key of the aromatic ring in the Met kinase binding.

Gratifyingly, the attempt to optimize the imidazonaphthyridinone-based type II Met inhibitors proved successful when utilizing the privileged structures presented by potent *c*-Met inhibitors entering clinical trials (Table 2, **3a–f**). For example, the fragment of *N,N'*-diphenyl cyclopropane-1,1-dicarboxamide was commonly present in type II *c*-Met kinase inhibitors such as **XL-184**, **XL-880**.<sup>11</sup> Furthermore, its conformationally constrained isostere, that is, *N*-phenyl-2-pyridone-3-carboxamide gave favorable

**Table 1**  
c-Met enzymatic activity of 3,5- and 1,8-disubstituted 1*H*-imidazo[4,5-*h*][1,6]naphthyridin-2(3*H*)-one derivatives as type I inhibitors<sup>a</sup>

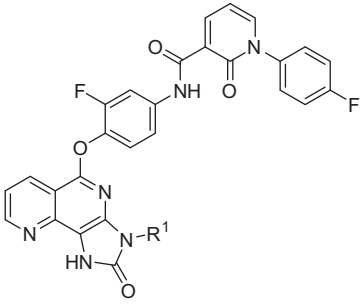


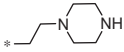
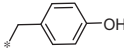
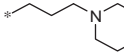
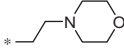
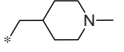
Compd	R <sup>1</sup>	R <sup>2</sup>	c-Met inhibition	
			% at 10 μM	IC <sub>50</sub> <sup>b</sup> (μM)
<b>1a</b>			33	—
<b>1b</b>			30.6	—
<b>1c</b>			65.8	26.0 ± 1.8
<b>1d</b>			37.4	—
<b>1e</b>			19.7	—
<b>1f</b>			39.7	—
<b>1g</b>			38.8	—
<b>2a</b>		-OH	21.2	—
<b>2b</b>			96.2	3.9 ± 0.2
<b>2c</b>			19.4	—
<b>2d</b>			44.9	12.7 ± 4.8
<b>2e</b>			6.4	—
<b>2f</b>			1.4	—
<b>2g</b>			15.7	—

<sup>a</sup> See [Supporting information](#) for the structural characterization of all tested compounds and a description of assay conditions.

<sup>b</sup> IC<sub>50</sub> values are reported as the mean of at least two independent determinations with eight concentrations each.

**Table 2**  
c-Met enzymatic activity and antiproliferative effect of 3,5-disubstituted-1*H*-imidazo[4,5-*h*][1,6]naphthyridin-2(3*H*)-one derivatives as type II inhibitors<sup>a</sup>



Compd	R <sup>1</sup>	c-Met inhibition		ECB-1 IC <sub>50</sub> <sup>c</sup> (μM)
		% at 10 μM	IC <sub>50</sub> <sup>b</sup> (μM)	
<b>3a</b>	H	20.3	—	—
<b>3b</b>		50.9	2.0 ± 0.1	>50
<b>3c</b>		51.5	3.6 ± 2.7	>50
<b>3d</b>		61.3	>50	—
<b>3e</b>		20.8	—	—
<b>3f</b>		42.7	2.9 ± 0.1	19.8 ± 1.2

<sup>a</sup> See Supporting information for the structural characterization of all tested compounds and a description of assay conditions.

<sup>b</sup> IC<sub>50</sub> values are reported as the mean of at least two independent determinations with eight concentrations each.

<sup>c</sup> Met-dependent human non-small lung cancer cell line, Met amplification.

c-Met inhibitory activity both in enzyme and cell levels.<sup>21</sup> Therefore, we directly appended the 2-pyridone-3-carboxamide moiety to the imidazonaphthyridinone core at C-5 position (Table 2), meanwhile slimming the original 1,3,5-trisubstitution core of lead **LXM-22** into 3,5-disubstitution one. When a hydrophilic heterocycle such as piperazine, piperidine or morpholine was attached on the N-3 position through an alkyl chain, the imidazonaphthyridinone-based type II inhibitors displayed low micromolar inhibitory activity against c-Met enzyme (Table 2, **3b**, IC<sub>50</sub> = 2.0 μM; **3c**, IC<sub>50</sub> = 3.6 μM; **3f**, IC<sub>50</sub> = 2.9 μM), providing a new motif for further structural optimization of type II c-Met kinase inhibitors.

The global structural exploration on the imidazonaphthyridinone-based c-Met kinase inhibitors identified an optimal motif bearing a pyridone-3-carboxamide pharmacophore at C-5 position and a hydrophilic heterocycle at N-3 position as type II inhibitors. However, this series of inhibitors gave disappointing results in the Met-driven ECB-1 cell proliferation assay (Table 2). The ECB-1 human lung cancer cell line expresses high levels of constitutively-activated Met kinase due to Met gene amplification.<sup>24,25</sup> According to the binding mode of the best compound **3f** in this series, predicted by the molecular modeling, the imidazolone moiety was involved in the H-bonding with the hinge region, but the moiety of 2-pyridone-3-carboxamide was not properly positioned in the DFG motif binding region (described in detail later in Figure 4 and the following binding mode interpretation). Therefore, further structural optimization was steered toward the re-shaping of the core and the side-chain structures.

Truncating the tricyclic core and replacing the rigid 2-pyridone-3-carboxamide fragment with a relatively flexible isostere of cyclopropane-1,1-dicarboxamide were performed for an improved activity (Table 3). Simply deduction of the pyridine ring from the

1*H*-imidazo[4,5-*h*][1,6]naphthyridin-2(3*H*)-one caused a big drop of the enzyme potency (Table 3, **4a**). But switching the dicarboxamide moiety from C-5 to C-7 position on the 1*H*-imidazo[4,5-*b*]pyridin-2(3*H*)-one core remarkably enhanced the Met kinase inhibition in both the biochemical and cell-based assays (**4b**, IC<sub>50</sub> = 209 nM, ECB-1 IC<sub>50</sub> = 240 nM). Synthetic attempt to introduce additional substituent on the imidazopyridine ring resulted in the formation of aminopyridine derivatives, which displayed improved biochemical potency but inferior cellular activity (**4c**, IC<sub>50</sub> = 19.5 nM, **4e**, IC<sub>50</sub> = 20.2 nM; ECB-1, 10 μM > IC<sub>50</sub> > 2 μM). The inconsistency between the enzyme and cellular potency might be attributed to the polar property of the molecule and thus poor cell membrane permeability. The fused piperidino benzimidazole analog gave similar biochemical inhibition (**4d**, IC<sub>50</sub> = 260 nM) but was 50-fold less potent in cells compared to the parent 1*H*-imidazo[4,5-*b*]pyridin-2(3*H*)-one inhibitor **4b**.

The cellular active inhibitors (**4b–c,e**) were further assessed for their ability to inhibit c-Met signaling in the Met-driven ECB-1 cells. Phosphorylation levels of the Met protein in ECB-1 cell lysates were determined by Western blotting after a 2 h incubation period. As illustrated in Figure 3, phosphorylation of the Met receptor was obviously inhibited by the selected compounds in a concentration-dependent manner, consistent with the observed antiproliferative activity in ECB-1 cells being a result of Met kinase inhibition. Furthermore, Erk1/2 and AKT, the key downstream molecules of c-Met that play important roles in Met-driven cellular proliferation and survival,<sup>4,26</sup> were also significantly inhibited as a result of our inhibitor treatment. These data support the finding that compounds **4b–c,e** inhibit c-Met signaling and, in turn, suppress c-Met dependent cell proliferation.

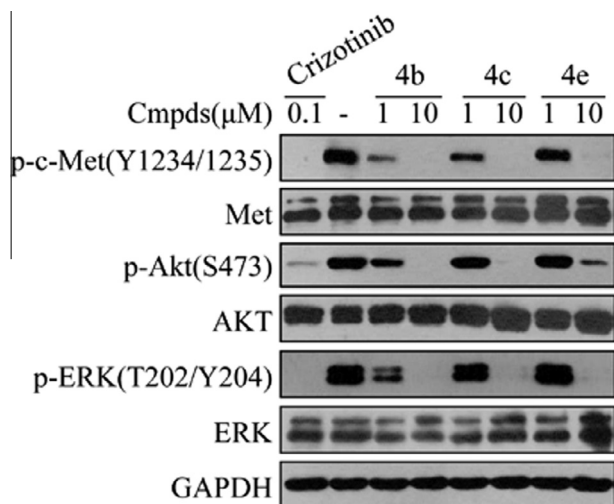
Since the parent 1*H*-imidazo[4,5-*h*][1,6]naphthyridin-2(3*H*)-one scaffold was disclosed to possess multiple kinase inhibitory activity,<sup>18</sup> we were interested in investigating the kinase selectivity of the newly developed 1*H*-imidazo[4,5-*b*]pyridin-2(3*H*)-one inhibitor. The lead compound **4b** was selected for kinase profiling against a panel of 15 oncogenic kinases (Table 4). Interestingly, at the concentration of 1 μM, **4b** was just effective in inhibiting the c-MET subfamily member RON and phylogenetically related kinase Axl, and EGFR, while it was almost inactive in all other 12 receptor and nonreceptor kinases in the panel. This result demonstrated the 1*H*-imidazo[4,5-*b*]pyridin-2(3*H*)-one scaffold achieved much higher Met kinase selectivity than the original 1*H*-imidazo[4,5-*h*][1,6]naphthyridin-2(3*H*)-one chemotype,<sup>18</sup> thus warranting a further preclinical development.

Based on the X-ray cocrystal structures of c-Met inhibitors bound to the Met kinase domain (PDB: 3CCN,<sup>27</sup> 3F82<sup>21</sup>), we established the binding modes of the new scaffold inhibitors (**2b**, **3f** and **4b**) by autodocking. As demonstrated by Figure 4, the 1,8-disubstituted-imidazonaphthyridinone based c-Met inhibitor **2b** binds to unphosphorylated c-Met kinase domain in a bend ‘U-shape’ conformation with the inhibitor wrapped around Met1211 as characteristic of type I inhibitor. The [1,6]naphthyridine core of **2b** is sandwiched into a narrow cleft formed by the P-loop of the N-lobe and the activation loop of the C-lobe, forming stable π–π stacking interaction with residue Tyr1230 and a H-bond between the carbonyl oxygen of [1,6]naphthyridine and the phenolic hydroxyl of Tyr1230. The 2-methoxy-pyridin-4-amine side chain faces to the solvent accessible region, and its amino unit makes an additional hydrogen bond with the carboxyl oxygen of residue Asp1164.

As type II c-Met inhibitors, compounds **3f** and **4b** also occupy the ATP-binding pocket but further extend into a second pocket that is formed by the residues of the activation loop in an inactive, DGF-out conformation. For compound **3f**, the *m*-fluoroaniline fragment resides in the middle of the tunnel between the hinge region and DFG motif. Aromatic ring of [1,6]naphthyridine forms stable π–π stacking interaction with residue Tyr1159. The

**Table 3**  
c-Met enzymatic and cellular activities of 1*H*-imidazo[4,5-*b*]pyridin-2(3*H*)-one derivatives as type II inhibitors<sup>a</sup>

Compd	Structure	c-Met inhibition		EBC-1 IC <sub>50</sub> <sup>c</sup> (μM)
		% at 1.0 μM	IC <sub>50</sub> <sup>b</sup> (nM)	
4a		33% @ 10 μM	–	–
4b		70	209 ± 45	0.24
4c		84	19.5 ± 2.0	<10
4d		71	260 ± 35	>10
4e		87	20.2 ± 3.7	<10

<sup>a</sup> See Supporting information for the structural characterization of all tested compounds and a description of assay conditions.<sup>b</sup> IC<sub>50</sub> values are reported as the mean of at least two independent determinations with eight concentrations each.<sup>c</sup> Met-dependent human non-small lung cancer cell line, Met amplification.**Figure 3.** Effects of the selected compounds on Met phosphorylation and downstream signaling in Met-driven lung cancer EBC-1 cells.

backbone carbonyl and N–H of residue Met1160 form two hydrogen bonds with the N–H of imidazole ring and nitrogen atom of [1,6]naphthyridine, respectively. The oxygen atom of pyridone fragment forms an additional hydrogen bond with backbone N–H of residue Asp1222. The *p*-fluoroaniline tail falls into the hydrophobic pocket formed by residues Ala1221, Leu1140, Val1139 and Leu1195 in DFG motif region. The potent and selective c-Met inhibitor **4b** adopts a similar binding pattern to **3f**. Significantly, the simplified 1*H*-imidazo[4,5-*b*]pyridin-2(3*H*)-one core is responsible for the strong interaction with c-Met by forming two

**Table 4**  
Effect of **4b** on a panel of PTKs at 1.0 μM concentration<sup>a</sup>

RTK	Inhibition rate (%)
Met	70 (IC <sub>50</sub> : 209 nM)
Ron	43.2
Axl	41.6
FGFR1	7.4
FGFR2	37.2
ALK	2.5
Flt-1	13.3
KDR	0.0
IGF1R	33.6
PDGFR-α	22.6
PDGFR-β	0.0
EGFR	49.5
ErbB4	24.3
c-Src	0.0
ABL	0.0
EPH-A2	18.8

<sup>a</sup> The kinase profiling assay was conducted by using ELISA kinase assay. Each reference compound and its inhibition rate for every kinase at the concentration of 1 μM (unless otherwise specified) was indicated below: XL-184 (0.1 μM) for RON (100%) and Axl (100%); AZD4547 (10 nM) for FGFR1 (95.1%) and FGFR2 (82.51%); AEW541 for IGF1R (56.6%); Su11248 for PDGFR-α (68.4%), PDGFR-β (80.2%), Flt-1 (66.6%), KDR (81.8%); BIBW2992 for EGFR (84.7%) and ErbB4 (84.2%); Dasatinib for c-Src (63.2%), ABL (56.7%) and EPH-A2 (76.2%).

hydrogen bonds with the hinge residue Met1160 as well as the pi-stacking interaction with Tyr1159. Furthermore, the two amide groups of the cyclopropane-1,1-dicarboxamide moiety are involved in three H-bonds with Asp1222 and Lys1110, which greatly enhances the potency. Hydrophobic interactions of the *p*-fluoroaniline moiety with DFG motif pocket also contribute to the tight binding.

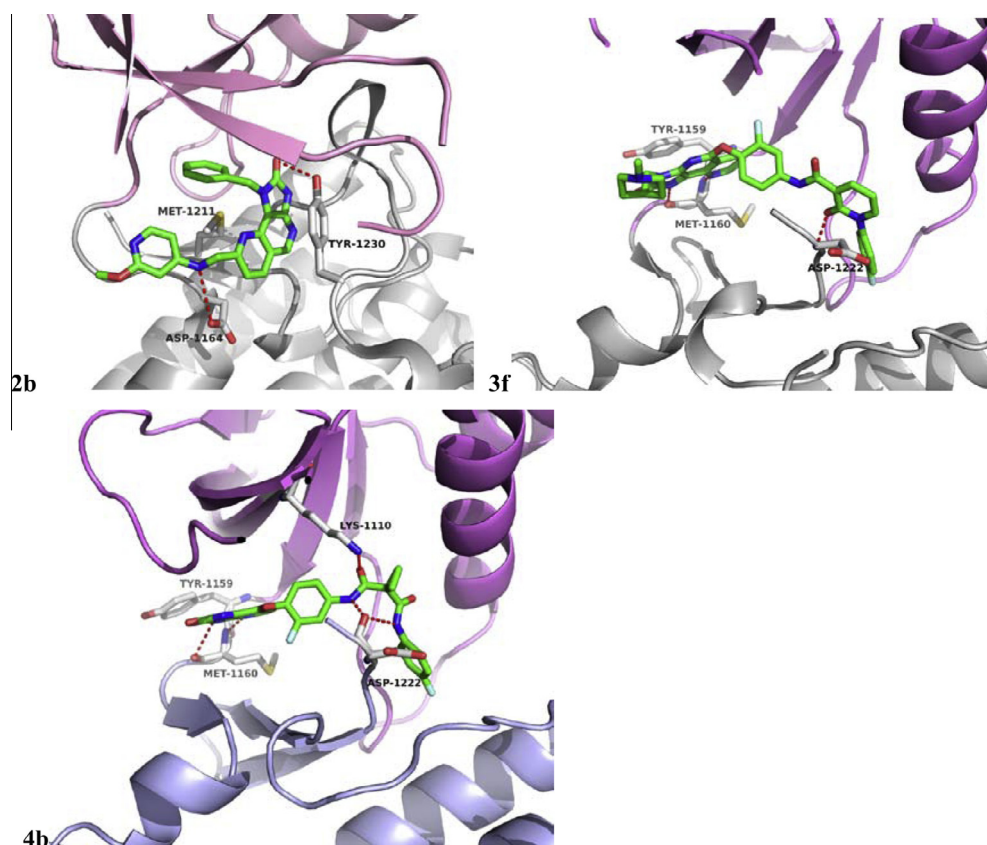


**Figure 4.** Proposed binding modes of selected compounds **2b**, **3f** and **4b** to the Met kinase domain, based on the X-ray co-crystal structure of c-Met in complex with a small molecule inhibitor.<sup>21,27</sup>

In conclusion, starting from our newly identified imidazonaphthyridinone c-Met inhibitors, based on the inhibitory mechanism, we conducted a global structural exploration with respect to the substitution pattern and the core structure size to furnish an optimal scaffold with improved potency and selectivity. A series of 3,5/1,8-disubstituted-1*H*-imidazo[4,5-*h*][1,6]naphthyridin-2(3*H*)-one derivatives were designed, synthesized and evaluated with privileged structures incorporated into N-1/C-8 or N-3/C-5 positions. 3,5-Disubstituted 1*H*-imidazo[4,5-*h*][1,6]naphthyridin-2(3*H*)-one turned out novel type II c-Met inhibitors with low micromolar IC<sub>50</sub> values. Further truncation of the core structure afforded potent and selective 1*H*-imidazo[4,5-*b*]pyridin-2(3*H*)-one Met inhibitors with nanomolar inhibition against the enzyme and the growth of Met-dependent EBC-1 human lung cancer cells, providing a promising new lead for further structural optimization and development of targeted cancer therapeutics.

#### Acknowledgments

This work was supported by grants from National Science Foundation of China (81325020, 21302201, 81321092 and 91229205), National Program on Key Basic Research Project of China (No. 2012CB910704), National S&T Major Projects of China (2012ZX09301001-007) and Science and Technology Commission of Shanghai Municipality, China (13ZR1447700).

#### Supplementary data

Supplementary data associated with this article can be found, in the online version, at <http://dx.doi.org/10.1016/j.bmcl.2014.11.070>.

#### References and notes

- Bottaro, D. P.; Rubin, J. S.; Falletto, D. L.; Chan, A. M. L.; Kmiecik, T. E.; Vandewoude, G. F.; Aaronson, S. A. *Science* **1991**, *251*, 802.
- Gherardi, E.; Birchmeier, W.; Birchmeier, C.; Woude, G. V. *Nat. Rev. Cancer* **2012**, *12*, 89.
- Naldini, L.; Vigna, E.; Narsimhan, R. P.; Gaudino, G.; Zarnegar, R.; Michalopoulos, G. K.; Comoglio, P. M. *Oncogene* **1991**, *6*, 501.
- Birchmeier, C.; Birchmeier, W.; Gherardi, E.; Vande Woude, G. F. *Nat. Rev. Mol. Cell Biol.* **2003**, *4*, 915.
- Migliore, C.; Giordano, S. *Eur. J. Cancer* **2008**, *44*, 641.
- Trusolino, L.; Bertotti, A.; Comoglio, P. M. *Nat. Rev. Mol. Cell Biol.* **2010**, *11*, 834.
- Comoglio, P. M.; Giordano, S.; Trusolino, L. *Nat. Rev. Drug Disc.* **2008**, *7*, 504.
- Engelman, J. A.; Zejnullahu, K.; Mitsudomi, T.; Song, Y. C.; Hyland, C.; Park, J. O.; Lindeman, N.; Gale, C. M.; Zhao, X. J.; Christensen, J.; Kosaka, T.; Holmes, A. J.; Rogers, A. M.; Cappuzzo, F.; Mok, T.; Lee, C.; Johnson, B. E.; Cantley, L. C.; Janne, P. A. *Science* **2007**, *316*, 1039.
- Straussman, R.; Morikawa, T.; Shee, K.; Barzily-Rokni, M.; Qian, Z. R.; Du, J. Y.; Davis, A.; Mongare, M. M.; Gould, J.; Frederick, D. T.; Cooper, Z. A.; Chapman, P. B.; Solit, D. B.; Ribas, A.; Lo, R. S.; Flaherty, K. T.; Ogino, S.; Wargo, J. A.; Golub, T. R. *Nature* **2012**, *487*, 500.
- Zhu, K. K.; Kong, X. Q.; Zhao, D.; Liang, Z. J.; Luo, C. *Expert Opin. Ther. Patents* **2014**, *24*, 217.
- Porter, J. *Expert Opin. Ther. Patents* **2010**, *20*, 159.
- Cui, J. J. *Expert Opin. Ther. Patents* **2007**, *17*, 1035.
- Liu, X. D.; Newton, R. C.; Scherle, P. A. *Expert Opin. Invest. Drugs* **2011**, *20*, 1225.
- Cui, J. J. *J. Med. Chem.* **2014**, *57*, 4427.
- Dussault, I.; Bellon, S. F. *Anti-Cancer Agents Med. Chem.* **2009**, *9*, 221.
- Berthou, S.; Aebersold, D. M.; Schmidt, L. S.; Stroka, D.; Heigl, C.; Streit, B.; Stalder, D.; Gruber, G.; Liang, C. X.; Howlett, A. R.; Candinas, D.; Greiner, R. H.; Lipson, K. E.; Zimmer, Y. *Oncogene* **2004**, *23*, 5387.
- Norman, M. H.; Liu, L. B.; Lee, M.; Xi, N.; Fellows, I.; D'Angelo, N. D.; Dominguez, C.; Rex, K.; Bellon, S. F.; Kim, T. S.; Dussault, I. *J. Med. Chem.* **2012**, *55*, 1858.
- Wang, Y.; Xu, Z. L.; Ai, J.; Peng, X.; Lin, J. P.; Ji, Y. C.; Geng, M. Y.; Long, Y. Q. *Org. Biomol. Chem.* **2013**, *11*, 1545.
- Williams, D. K.; Chen, X. T.; Tarby, C.; Kaltenbach, R.; Cai, Z. W.; Tokarski, J. S.; An, Y. M.; Sack, J. S.; Wautlet, B.; Gullo-Brown, J.; Henley, B. J.; Jeyaseelan, R.; Kellar, K.; Manne, V.; Trainor, G. L.; Lombardo, L. J.; Fargnoli, J.; Borzilleri, R. M. *Bioorg. Med. Chem. Lett.* **2010**, *20*, 2998.

20. Zeng, L. F.; Wang, Y.; Kazemi, R.; Xu, S. L.; Xu, Z. L.; Sanchez, T. W.; Yang, L. M.; Debnath, B.; Odde, S.; Xie, H.; Zheng, Y. T.; Ding, J.; Neamati, N.; Long, Y. Q. *J. Med. Chem.* **2012**, *55*, 9492.
21. Schroeder, G. M.; An, Y. M.; Cai, Z. W.; Chen, X. T.; Clark, C.; Cornelius, L. A. M.; Dai, J.; Gullo-Brown, J.; Gupta, A.; Henley, B.; Hunt, J. T.; Jeyaseelan, R.; Kamath, A.; Kim, K.; Lippy, J.; Lombardo, L. J.; Manne, V.; Oppenheimer, S.; Sack, J. S.; Schmidt, R. J.; Shen, G.; Stefanski, K.; Tokarski, J. S.; Trainor, G. L.; Wautlet, B. S.; Wei, D.; Williams, D. K.; Zhang, Y. R.; Zhang, Y. P.; Fargnoli, J.; Borzilleri, R. M. *J. Med. Chem.* **2009**, *52*, 1251.
22. Wang, Y. X.; Ai, J.; Wang, Y.; Chen, Y.; Wang, L.; Liu, G.; Geng, M. Y.; Zhang, A. J. *Med. Chem.* **2011**, *54*, 2127.
23. Zhang, D. Y.; Ai, J.; Liang, Z. J.; Zhu, W.; Peng, X.; Chen, X. J.; Ji, Y. C.; Jiang, H. L.; Luo, C.; Geng, M. Y.; Liu, H. *Bioorg. Med. Chem. Lett.* **2013**, *23*, 2408.
24. Park, M.; Dean, M.; Cooper, C. S.; Schmidt, M.; Obrien, S. J.; Blair, D. G.; Vandewoude, G. F. *Cell* **1986**, *45*, 895.
25. Sattler, M.; Pride, Y. B.; Ma, P.; Gramlich, J. L.; Chu, S. C.; Quinnan, L. A.; Shirazian, S.; Liang, C. X.; Podar, K.; Christensen, J. G.; Salgia, R. *Cancer Res.* **2003**, *63*, 5462.
26. Bertotti, A.; Burbridge, M. F.; Gastaldi, S.; Galimi, F.; Torti, D.; Medico, E.; Giordano, S.; Corso, S.; Rolland-Valognes, G.; Lockhart, B. P.; Hickman, J. A.; Comoglio, P. M.; Trusolino, L. *Sci. Signal.* **2009**, *2*, ra80.
27. Albrecht, B. K.; Harmange, J. C.; Bauer, D.; Berry, L.; Bode, C.; Boezio, A. A.; Chen, A.; Choquette, D.; Dussault, I.; Fridrich, C.; Hirai, S.; Hoffman, D.; Larrow, J. F.; Kaplan-Lefko, P.; Lin, J.; Lohman, J.; Long, A. M.; Moriguchi, J.; O'Connor, A.; Potashman, M. H.; Reese, M.; Rex, K.; Siegmund, A.; Shah, K.; Shimanovich, R.; Springer, S. K.; Teffera, Y.; Yang, Y. J.; Zhang, Y. H.; Bellon, S. F. *J. Med. Chem.* **2008**, *51*, 2879.